

Cell Reports, Volume 29

Supplemental Information

***henn-1/HEN1* Promotes Germline**

Immortality in *Caenorhabditis elegans*

Joshua M. Svendsen, Kailee J. Reed, Tarah Vijayasathy, Brooke E. Montgomery, Rachel M. Tucci, Kristen C. Brown, Taylor N. Marks, Dieu An H. Nguyen, Carolyn M. Phillips, and Taiowa A. Montgomery

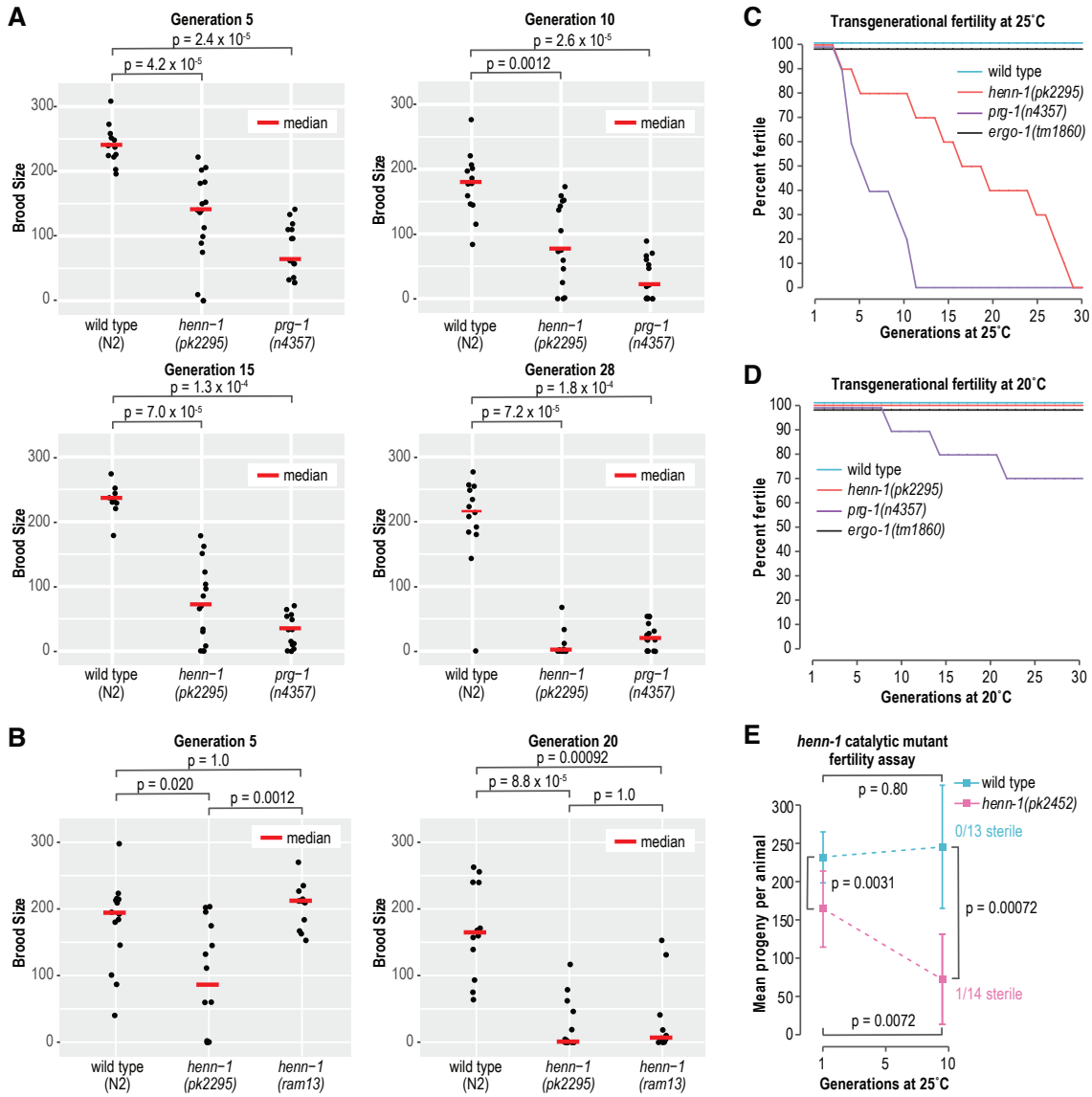


Figure S1. Related to Figure 1. *henn-1* transgenerational fertility assays. (A) Brood sizes of wild type, *henn-1*(pk2295), and *prg-1*(n4357) at ~5, ~10, ~15, and ~28 generations. Bonferroni adjusted p values were calculated using Wilcoxon rank-sum tests. Each data point represents the number of progeny produced by one animal. Results summarized in Figure 1A. (B) Brood sizes of wild type, *henn-1*(pk2295), and *henn-1*(ram13) at ~5 and ~20 generations. Bonferroni adjusted p values calculated using Wilcoxon rank-sum tests. Results summarized in Figure 1B. (C-D) Percentages of 10 independent lines of wild type, *henn-1*(pk2295), *prg-1*(n4357), and *ergo-1*(tm1860) that remained fertile at each generation at 25°C (C) and 20°C (D). Animals that produced any progeny were considered fertile. (E) Brood sizes of wild type and *henn-1*(pk2452) (catalytic domain mutant) at 1 generation (wild type, n = 15; *henn-1*, n = 13) and 10 generations (wild type, n = 13; *henn-1*, n = 14) at 25°C. The numbers of sterile animals at 10 generations are shown. Bonferroni adjusted p values were calculated using Wilcoxon rank-sum tests.

Overlap in WAGO-class 22G-RNAs
depleted in *henn-1* and *prg-1*

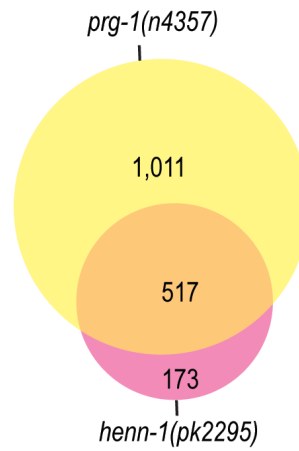


Figure S2. Related to Figure 2. Most *henn-1*-dependent 22G-RNAs are derived from piRNA targets. The Venn diagram displays overlap in WAGO-class 22G-RNAs that are depleted >50% in *henn-1*(pk2295) and *prg-1*(n4357) adult whole animals relative to wild type.

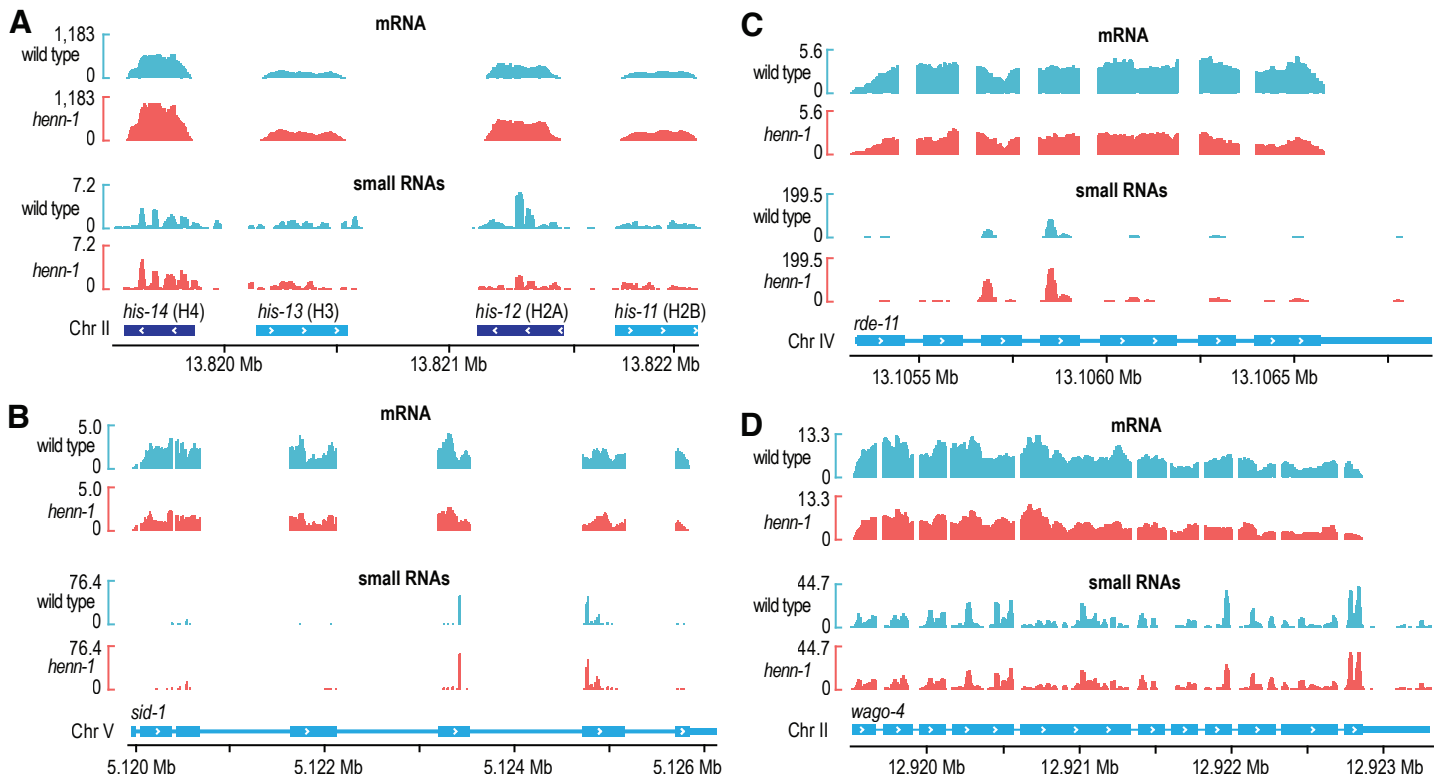


Figure S3. Related to Figure 3. Small RNA and mRNA misregulation in *henn-1* mutants. (A) mRNA and small RNA read distribution across a histone cluster in wild type and *henn-1(pk2295)*. (B) mRNA and small RNA read distribution across *sid-1* in wild type and *henn-1(pk2295)*. (C) mRNA and small RNA read distribution across *rde-11* in wild type and *henn-1(pk2295)*. (D) mRNA and small RNA read distribution across *wago-4* in wild type and *henn-1(pk2295)*. Plots were generated in IGV.

siRNA enrichment following oxidation

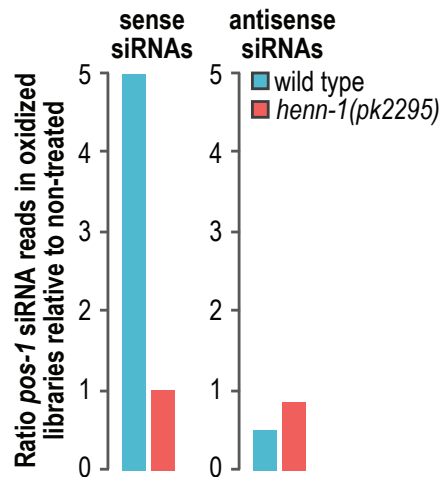


Figure S4. Related to Figure 4. *henn-1* is required for primary siRNA methylation. Bar plots display the ratio of normalized reads mapping to *pos-1* in sodium periodate treated (oxidation +) and control treated (oxidation -) wild type and *henn-1(pk2295)* small RNA libraries. The left plot includes only sense-mapping reads to *pos-1*, which are presumably primary siRNAs. The right plot includes only antisense siRNAs, which are predominantly secondary siRNAs (22G-RNAs).

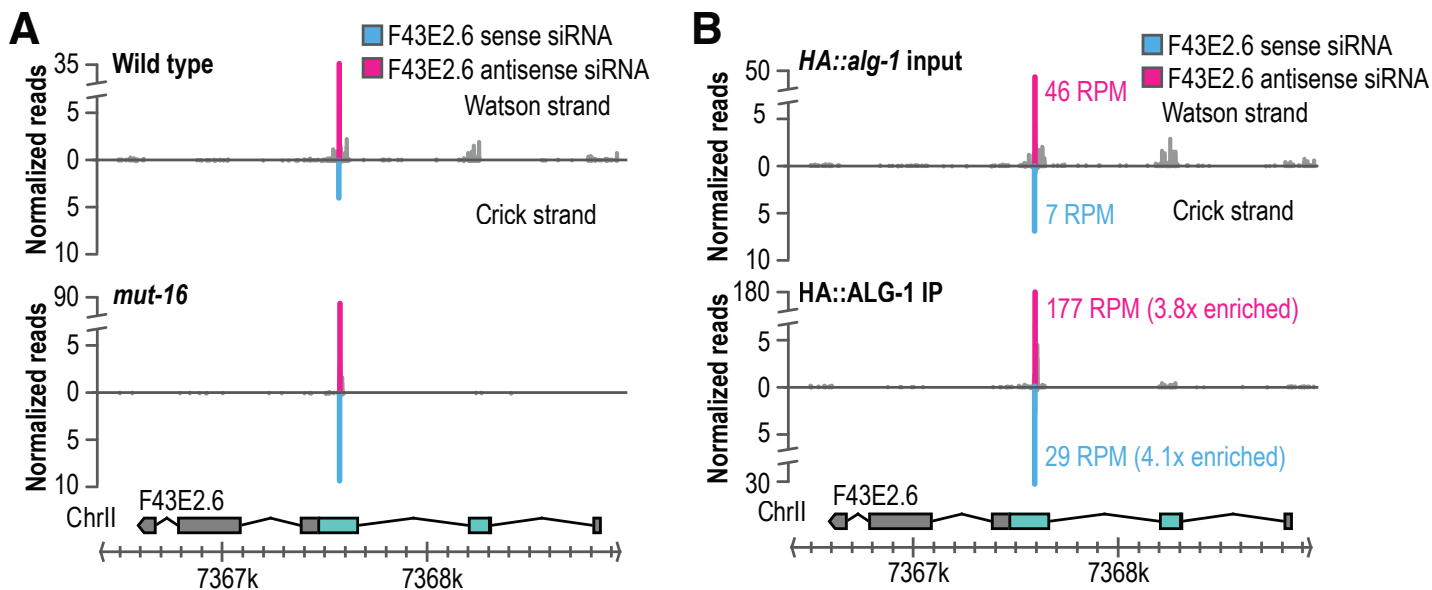


Figure S5. Related to Figure 5. F43E2.6 is a *mut-16*-independent siRNA locus. (A) Normalized read distribution across the F43E2.6 siRNA-generating locus in wild type (upper panel) and *mut-16*(*pk710*) (lower panel). Sense siRNA reads are in blue and antisense are in magenta. (B) Normalized read distribution (reads per million total, RPM) across the F43E2.6 siRNA-generating locus from *HA::alg-1* cell lysate (upper panel) and *HA::ALG-1* co-IP (lower panel). Fold enrichment in *HA::ALG-1* co-IP relative to cell lysate is shown.